Finite Element Model of a Fetal Skull Subjected to Labour Forces

R. J. Lapeer and R. W. Prager

Department of Engineering, Cambridge University, Cambridge, UK

Abstract. The objective of this research is to study the deformation of a human fetal skull when subjected to labour forces. The shape of the fetal skull is recovered from a laser-scanned replica model. A combined technique of thin-plate spline surface fitting and an advancing front triangulation method provide a valid mesh model for finite element analysis. The skull is assumed to be a shell object and contains about 64,000 shell elements. The area around the parietal bones is subjected to a pressure load, exerted by the uterine cervix during the first stage of labour. The analysis investigates the influence of four parameters in the model. The resulting deformations agree with previous findings in terms of shape of deformation but are smaller in terms of degree of deformation. This may imply that moulding of the fetal skull during the birth process cannot be solely modelled by the short-time effect of a static load but effects such as hyper-elastic behaviour of the sutures, visco-elastic behaviour of the cranial bones and sliding contact between the head and surrounding tissues should be considered.

1 Introduction

In obstetrics, mechanical concepts are undeniably of major importance. Despite being applied for more than a century, for example the use of mechanical tools such as the forceps and more recently the vacuum extractor for operative delivery, these concepts are usually based on *mechanisms* of labour rather than *mechanics* of labour [1]. Mechanisms of labour are primarily concerned with fetal *movements* of which the majority occur in the second stage of labour. Mechanics of labour is however a much wider concept, involving both the first and second stage of labour and focusing on theoretical mechanical concepts rather than practical issues which are aimed at the delivery of the baby.

From as early as 1861, Kristeller ([1]) attempted to measure the forces during labour by inserting balloons into the uterus via the vagina. Many investigations to measure the forces, and more specific the amniotic pressure and the pressure between the fetal head and the cervix during the first stage, have followed since. The most recent results, amongst many, are from Lindgren [2], Rempen [3] and Antonucci [4].

Bell [1] gave an excellent overview in the early 70's on the mechanical issues of

C. Taylor, A. Colchester (Eds.): MICCAI'99, LNCS 1679, pp. 1143–1155, 1999.
© Springer-Verlag Berlin Heidelberg 1999

human parturition. His work is an invaluable contribution since it covers possibly all the work done until 1972.
In the early 90's, the *computerised birth simulation* became a fashionable topic. Wischnik et al. [5] simulated birth by reconstructing the geometry of the birth canal and the fetal head by means of MRI images and the Marching Cubes algorithm [6]. Similar work was done by Geiger [7] and later on by Liu et al. [8]. The idea behind a birth simulation is to allow an obstetrician to assess the probability of a successful vaginal delivery a sufficient time before the actual event. The simulation could for example indicate possible complications such as *cephalo-pelvic disproportion*. This would allow the obstetrician to plan an *elective Caesarian section* rather than risking an *emergency Caesarian section* at the time of delivery. One important issue which was not covered in depth in the work of Wischnik, Geiger and Liu is the moulding of the fetal skull during delivery.
McPherson and Kriewall performed invaluable research in 1980 regarding the biomechanics of fetal head moulding. They evaluated the elasticity modulus of fetal cranial bone from seven stillborn babies [9] and analysed the behaviour of the parietal bones when subjected to the amniotic pressure, AP, and the head-to-cervix pressure, HCP, using a finite element model [10].
A realistic model of the biomechanical behaviour of the fetal skull when subjected to labour forces would allow to significantly improve the reliability and accuracy of a computerised simulation of birth and would also contribute to the investigation of *post-natal pathological conditions* caused by *excessive head moulding*.
The objective of this research is to improve this model by extending the analysis on the parietal bones as performed by McPherson and Kriewall to the fetal skull in its entirety. This requires a more accurate shape model and a more detailed analysis of deformation because of increased complexity.

2 Shape Recovery and Mesh Generation

2.1 Data Acquisition

Considering the fact that the cranial bones of the fetal skull are very thin compared to their surface dimensions [9], a shell-based model is justified[1]. Thus, the reconstruction of the outer surface would be sufficient to build a finite element mesh model composed of shell elements.
A surface model of a fetal skull was derived from laser-scanning a life-size model of a real fetal skull, designed and manufactured by ESP Ltd.
The purpose-built laser scanner from the Dept. of Medical Physics at UCL was developed for the simulation of maxillo-facial surgery [12]. A beam of laser light is fanned out into a line and projected onto the object surface. When the line is viewed obliquely by a CCD camera it is curved, reflecting the shape of the surface at the intersection with the laser beam. The scanned object is placed on

[1] This abstraction has even been used to model adult skulls as reported by Hosey [11].

a turntable hence a matrix of data points around the surface is obtained. The collected data usually consists of between 20,000 and 60,0000 3D coordinates of points lying on the anatomical surface. Individual points can be recorded with a precision better than 0.5 mm. The triangulation of the data points is straightforward because they form an ordered grid of points. One shortcoming of the laser-scanning system is the inability to scan the top and bottom part of the object. This requires the acquisition of several datasets to obtain data across the entire object. Furthermore, the acquisition suffers from bad connections (triangles with high aspect ratio) because data points are missing in concavities, noise due to interfering objects such as the supporting table, incorrect surface patterns because of vibrations and an unclosed gap between the first and last array of scanned points. In total, four datasets were acquired. To arrive at a single, complete and valid shape/mesh model the following operations were necessary:

1. Noise removal for each selected dataset: a customised software tool, the interactive mesh-modelling toolkit (*immtk*) allows easy removal of noise.
2. Registration of the selected datasets: based on the conventional approach of landmark matching followed by least-squares parameter estimation of an affine transformation.
3. Selection of valid parts of each selected dataset, resulting in a set of registered, unconnected patches (Figure 1a).
4. Connection of the loose parts and interpolation of sections of missing data, to obtain a valid and complete mesh model. The methodology is outlined in the next section.

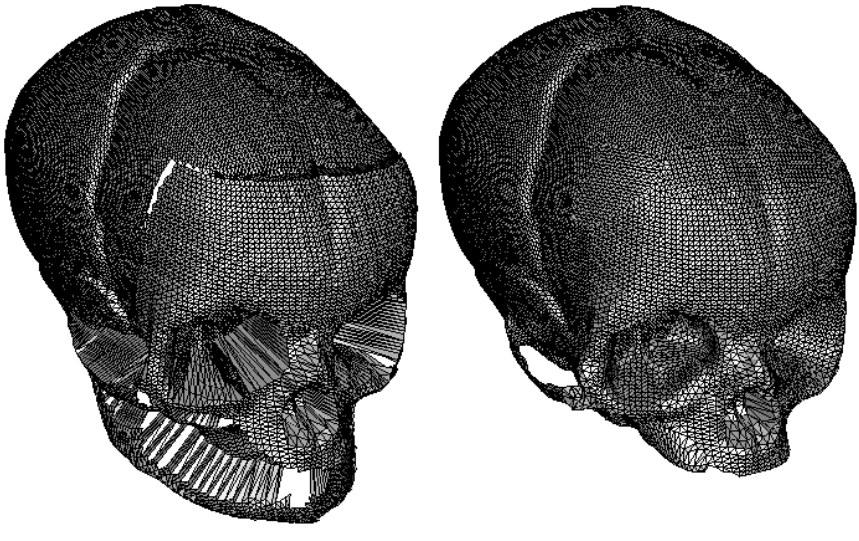

(a) Unconnected, raw mesh model (b) Final mesh model

Fig. 1. Skull models before and after surface interpolation and remeshing.

2.2 Surface Interpolation, Mesh Generation and Mesh Optimisation

Thin-Plate Spline Surface Interpolation The thin-plate spline model is ideal for surface interpolation, when a significant part of the surface data is missing or invalid, because it minimises bending energy. An explicit thin-plate spline surface with radial basis function [13] is defined as :

$$z = f(x, y) = -U(r) = -r^2 \log(r^2) \tag{1}$$

where the coefficient of the radial basis function

$$r = \sqrt{(x^2 + y^2)} \tag{2}$$

The thin-plate spline surface parameters can be obtained from a set of valid data points on an unconnected or falsely connected patch, selected by the user.

Surface Patch Triangulation The first algorithm involves triangles *growing* from the centre of the surface towards the outer boundary Γ. The *invariant* of the algorithm ensures that generated triangles do not penetrate the boundary. When the *post-condition* is reached, i.e. no triangles can be further expanded, an internal boundary is created from the interior triangles. A second algorithm, which we call the *welding* algorithm, connects the interior boundary to the original boundary Γ. The welding algorithm is based on the *advancing front principle*. The advancing front principle was originally developed by Lo [14] and has since widely been used in algorithms for finite element mesh generation and adaptation.

Mesh Optimisation and Refinement In finite element analysis (FEA), it is important that the elements in the mesh have a good aspect ratio to minimise numerical errors during the calculation of the stiffness matrix and the element normals.
The aspect ratio, ar, of a triangle can be defined as the ratio of the longest edge and the perpendicular distance from this edge to the opposite triangle vertex. The best aspect ratio is exhibited by the equilateral triangle: $ar = 1.1547$. Two simple approaches to optimise the aspect ratio of the mesh are the adjustment of a vertex towards the centre of its surrounding polygon on the surface, also known as Laplacian smoothing, and edge swapping. NAFEMS [15] advises: $ar \leq 4$.
Another important concept in FEA is the number of elements in the mesh model. This parameter is crucial to the accuracy of the solution of the analysis, as the latter converges to the exact solution of the problem, as the number of elements is increased [16]. Cubic spline interpolation of the boundary edges allows the creation of new vertices at arbitrary distances on the boundary. The algorithm described in the previous section can thus generate meshes of arbitrary refinement.

Results Figure 2 shows meshes of a parietal bone [17]: The original mesh (a), the optimised mesh using Laplacian smoothing and edge swapping (b) and a newly created mesh with refinement (c).
Figure 1b shows the connected and optimised mesh of the fetal skull.

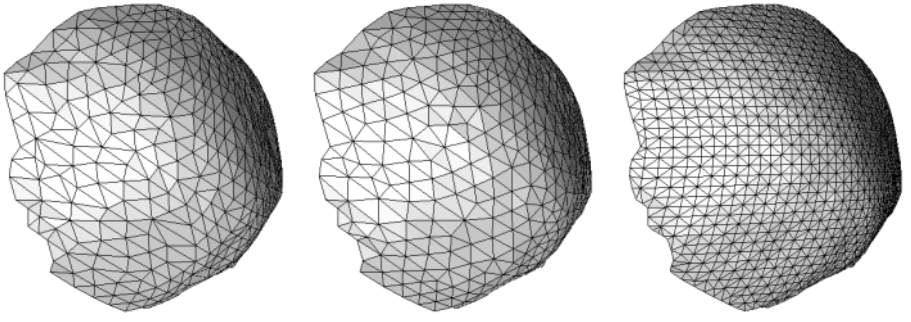

(a) Original mesh (b) Smoothed mesh (c) Refined mesh

Fig. 2. Mesh models of a parietal bone.

3 Finite Element Analysis of the Fetal Skull

3.1 General Concepts

The accurate description of a physical problem using a finite element model is sensitive to an array of possible errors [18]:

- Modelling error: Whatever the analysis method, we do not analyse the actual physical problem but the mathematical model of it. To arrive at such a model, we make assumptions which do not always reflect the exact behaviour of the problem.
- Numerical error: The numerical output has been rounded and truncated during the course of the analysis. Numerical errors are usually small but some modelling practises can significantly increase them.
- Discretisation error: The physical structure which we analyse and the mathematical model have infinitely many degrees of freedom (d.o.f.) whilst the finite element model has a finite number of d.o.f. This implies that the discretisation error will tend to zero as the number of elements increases but will never become zero.

3.2 Experiment: Initial Setup

The ABAQUS/Standard software was used to perform the analysis.

Geometry:

- The fetal skull model contains 63,413 elements which is sufficient to describe the geometry of the skull in detail (average triangle dimensions < 1 mm.) and the field variable under investigation, i.e. deformation.
- The mandible is left out since it is not a fixed part of the cranium and is unlikely to contribute to the moulding process.
- The thickness of the shells of the cranial vault is initially set to 0.75 mm., an average value of the thickness of parietal and frontal bones as reported in [10].
- The thickness of the maxilla, palate and skull base is set to 2 mm. - an estimate based on the thickness of the palate of the fetal skull model.
- The thickness of the fontanelles is initially set to 0.75 mm. - the same value as for the cranial bones.

Direction of the axes: See Figures 4 and 5a.

Elements: Constant strain elements (ABAQUS S3R) for both the fontanelle/suture structures and the bones of the fetal skull. The S3R shell element in ABAQUS provides accurate results in most loading situations and is valid for thin- and thick-shell problems. However, due to its constant bending and membrane strain approximations, high mesh refinement is required to capture pure bending deformations or solutions to problems of high strain gradients. The bones of the cranial vault, i.e. parietal and frontal bones, temporal bones and occipital bone, are modelled with thin-shell elements. Figure 3 shows a view of the skull base which is composed of thick-shell elements to emulate its stiffer behaviour.

Material properties: Based on findings reported by McPherson and Kriewall [9].

- Fetal cranial bone (at term)[2]: orthotropic, plane stress, $E_1 = 3.86\text{e}3$ MPa, $E_2 = 0.965\text{e}3$ MPa, $G_{12} = 1.582\text{e}3$ MPa, $G_{13} = G_{23} = 1.582\text{e}3$ MPa, $\nu = 0.08$
- Fontanelles and sutures: isotropy assumed, $E = 31.5$ MPa, $\nu = 0.45$, values of the properties of the dura mater as reported by McElhaney [19].

Boundary conditions: Three nodes at the base of the skull, located at the left and right tympanic ring and the middle of the palate respectively are fully built-in to avoid rigid body displacement. Three extra nodes on the maxilla to avoid rotation about the x-axis.

[2] E_i is Young's modulus in the ith local direction, G_{ij} is the shear modulus in the plane with normal in the ith local direction and force in the jth direction, ν is Poisson's ratio.

Loads: The loading of the skull is modelled at the first stage of labour where the head is in contact with the cervix. The pressures are average values based on values reported in [2,3,4]:

- amniotic pressure, AP: 50 mmHg. - above the suboccipito-bregmatic plane,
- head-to-cervix pressure, HCP: 250 mmHg. - below the suboccipito-bregmatic plane.

Figure 4 shows the pressure distribution: the light-coloured area above the SOB plane (positive z-direction) is subjected to amniotic pressure. The dark-coloured band just below the SOB plane (negative z-direction) is the head-to-cervix pressure. The light-coloured area beyond the high pressure region is not subjected to any loading.

Analysis: Static analysis assuming non-linear geometry.

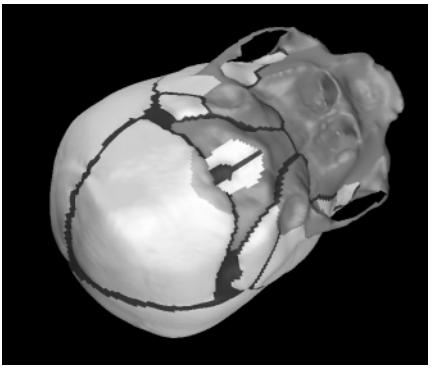

Fig. 3. Fetal skull base: The dark-grey region is composed of thick-shell elements.

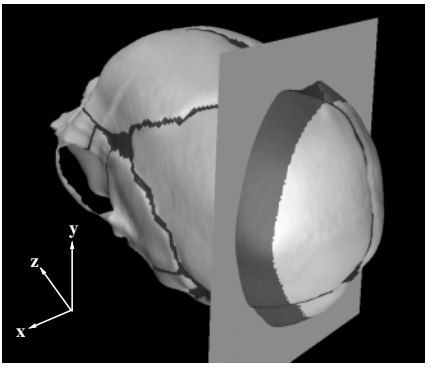

Fig. 4. Pressure distributions - AP: above the SOB plane; HCP: dark-coloured band below the SOB plane.

3.3 Objectives

In this preliminary experiment we aim to assess the deformation of the bones of the cranial vault. McPherson and Kriewall [10] analysed the deformation of the parietal bones when subjected to the amniotic pressure and cervical pressure during the first stage of labour.
The current analysis extends the investigation to the behaviour of the entire skull and assesses the sensitivity of the results towards changes of the thickness of the bones and sutures, the elasticity and shear moduli and the pressure. Table 1 reports the parameter settings for each analysis. The first analysis is based

on the average values as reported earlier. In subsequent analyses, the values of the elasticity and shear moduli, shell thickness and maximum pressure are set to such boundary values, within their valid range, as to increase the moulding effect.
Evaluations are based on measurements of the bi-parietal diameter, BPD, the sub-occipito bregmatic diameter, $SOBD$, the orbito-vertical diameter, $OrVD$ and the maxillo-vertical diameter, $MaVD$, before and after moulding (See Figure 5).

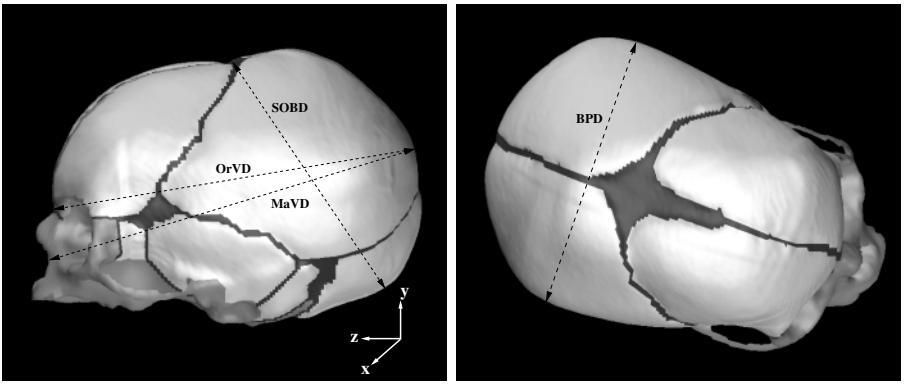

(a) (b)

Fig. 5. Diameters for evaluation of fetal skull moulding.

Table 1. Analysis parameters.

Analysis	E_1 (MPa)	E_2 (MPa)	G_{12} (MPa)	G_{13} (MPa)	thickness bone (mm)	thickness sut/font (mm)	HCP (MPa)
1	3.860E3	0.965E3	1.582E3	1.582E3	0.750	0.750	-33.33E-3
2	2.830E3	0.570E3	1.160E3	1.160E3			
3	3.860E3	0.965E3	1.582E3	1.582E3		0.375	
4					0.600	0.600	
5					0.750	0.750	-53.28E-3

3.4 Results

Table 2 reports:

– The values of the BPD, $SOBD$, $OrVD$ and $MaVD$ as reported by Sorbe and Dahlgren [20]: they performed a clinical trial on 319 deliveries, without complications, measuring the diameters shortly after birth and three days later. If we consider restitution of the skull as the inverse process of moulding then the diameters measured after three days correspond to the original

dimensions whilst those measured shortly after birth correspond to the dimensions after moulding. In Table 2, row 0 reports the *original* diameters; row 1 reports the elongation(+) or compression(-) after moulding[3].
- The values of the BPD, $SOBD$, $OrVD$ and $MaVD$ as a result of our analysis. Row 0 reports the original diameters[4]. Subsequent rows report the strain after moulding for each analysis as reported in Table 1.
- All reported values are in mm.

Figure 6 shows the shape of the skull before and after deformation (deformation magnification = 10.0).

Table 2. Strains of four main diameters (mm.) of the fetal skull. Own results, L-P, are compared with results from S-D [20].

Diameter	S-D(0)	S-D(1)	L-P(0)	L-P(1)	L-P(2)	L-P(3)	L-P(4)	L-P(5)
BPD	105.00	0.00	89.75	-0.07	-0.05	-0.21	-0.11	-0.03
$SOBD$	117.10	-1.70	88.71	-0.36	-0.42	-1.07	-0.68	-0.63
$OrVD$	126.90	+2.20	119.35	+0.10	+0.13	+0.25	+0.20	+0.17
$MaVD$	140.50	+1.90	129.28	+0.13	+0.15	+0.30	+0.24	+0.20

4 Discussion

Before we compare the results of our simulation with the measurements from Sorbe and Dahlgren, we first discuss the effects of the change of parameters amongst the different analyses[5], as shown in the lower section of Table 2:

- In analysis 3, the fontanelle/suture thickness was set to a lower bound based on values as reported in [21]. It appears to have the most significant effect to the stiffness of the skull. This observation is to some degree supported by the results from analysis 4.
- Changing the stiffness parameters of the cranial bones to a lower bound (analysis 2) does not seem to have a major effect. The explanation lies in the inherent stiffness of a shell-shaped object.
- Finally, the increase of the head-to-cervix pressure to a value of 400 mmHg. (analysis 5) has a significant effect on all diameters except on the BPD. A possible explanation, similar to the previous one, is based on the stiffness of a shell: the BPD is measured near to, or possibly exactly on, the parietal

[3] In the further course of this text we will refer to elongation/compression as *strain*. This variable is however not the same as the strain, ϵ, which is commonly used in stress analysis and is dimensionless.

[4] The diameters as measured by Sorbe and Dahlgren are larger because of the skin!

[5] Remember: Analysis 1 involves the initial settings.

tuberosities. The latter display the highest curvature of the parietal bone, hence increasing the pressure will have less effect than for example decreasing the bone thickness (analysis 4).

The resulting strains are direction-wise (i.e. elongation vs compression) in complete agreement with the measurements from Sorbe and Dahlgren [20] for the $SOBD$, $MaVD$ and $OrVD$: the $SOBD$ decreases during moulding whilst the $MaVD$ and $OrVD$ decrease. The magnitudes are however significantly smaller for the $MaVD$, $OrVD$ and $SOBD$, the latter to a lesser extent for the configuration of analysis 3. Possible explanations are:

- Effects such as hyper-elastic behaviour of the fontanelles/sutures [21] and visco-elastic behaviour of the skull bones [22] have not been considered. These effects would increase the strains significantly under the same material properties and loading conditions.
- The variable thickness of the skull as reported in [9,10], varying from higher values at the ossification centres of the bone to lower values at the periphery, will decrease the overall stiffness.
- The measurements reported by Sorbe and Dahlgren [20] are not entirely accurate:
  - Measurements as reported in Table 2 were performed by a photographic method. The advantage of this procedure, as opposed to the use of obstetric callipers, is the elimination of the effect of the skin, the latter resulting in a significant underestimate of the true value. The drawback however is the inability to correctly position the skull, hence parallax errors on the measurements result.
  - The inter-observer variance (from ten different observers on a single child) was 2.7 mm. for the $SOBD$, 2.1 mm. for the BPD, 2.8 mm. for the $OrVD$ and 2.3 mm. for the $MaVD$.

Sorbe and Dahlgren did not find significant changes for the BPD. Our results show a small decrease of the BPD, significant though because of the non-stochastic nature of our 'measurements'.
Figure 6 shows the lifting of the parietal bones when subjected to the cervix pressure. This phenomenon is commonly known by obstetricians and paediatricians and has also been reported in [10] and [23]. However, the figure shows that the frontal bones lift as well. Since they are mainly subjected to the amniotic pressure, some of the effect might come from the parietal bones.

5 Conclusion

An accurate model on the behaviour of the fetal skull during and shortly after delivery is of major importance to the obstetric and paediatric community. We presented a preliminary analysis on this behaviour by assessing the deformation of a fetal skull when subjected to pressures during the first stage of labour.
The shape of the skull was acquired from laser-scanned data. The acquisition

of a CT dataset, though difficult to obtain for a healthy newborn, could be an improvement in terms of more accurate modelling of the internal structures of the skull[6].

The combined surface interpolation/mesh generation method allows us to create a valid, compatible and optimised mesh-model. This method works well for level surfaces but further improvement towards a fully 3D implementation should be considered to avoid 'patching' of general 3D surfaces such as the skull.

The results of the FEA do correspond with measurements as reported in [20] in terms of *shape of deformation*, however, the *degree of deformation* is significantly lower. Possible explanations to the *over-stiffness* of our model were mentioned in the previous section.

The model as presented in this study, despite being significantly more accurate than the previous model of McPherson and Kriewall [9], can still be considerably improved by:

- consideration of the skin: the elastic properties of the skin would reduce the effect of the pressures on the cranium,
- consideration of the incompressibility of the brain: the model should include a parameter to allow for deformation without change of volume,
- the effect of the entire dura mater rather than fontanelles and sutures only,
- geometric modelling of the inner structures of the skull from data obtained from a CT dataset of a fetal or newborn head,
- more reliable values of material constants and dimensions,
- more accurate measurements of pressure distributions as exerted on the fetal skull, during the first and second stage of labour,
- the consideration of the second stage of labour, when the fetal head is in contact with the soft tissues of the birth canal and the bony pelvis,
- to model the problem using *sliding contact* analysis rather than *static* analysis.

Fetal head moulding is a phenomenon with both positive and negative aspects. The positive aspect manifests itself during the birth process where the moulding of the skull allows the fetus to pass through the birth canal even when the dimensions of the latter are restricted. On the contrary, excessive head moulding can result into pathological conditions, shortly after birth or even a long term thereafter. A realistic model of the biomechanical behaviour of the fetal skull when subjected to labour forces would significantly improve the *sensitivity* and *specificity* of a *computerised simulation of birth*, used as a tool for timely decision on mode of delivery. It would also contribute to the investigation of *post-natal pathological conditions* caused by *excessive head moulding*.

The model as presented in this paper is therefore a big step forwards into a better understanding of the *mechanics of fetal head moulding* and its potential applications.

[6] Care should be taken however since the resolution of conventional CT images is of the order of magnitude of the thickness of the cranial bone.

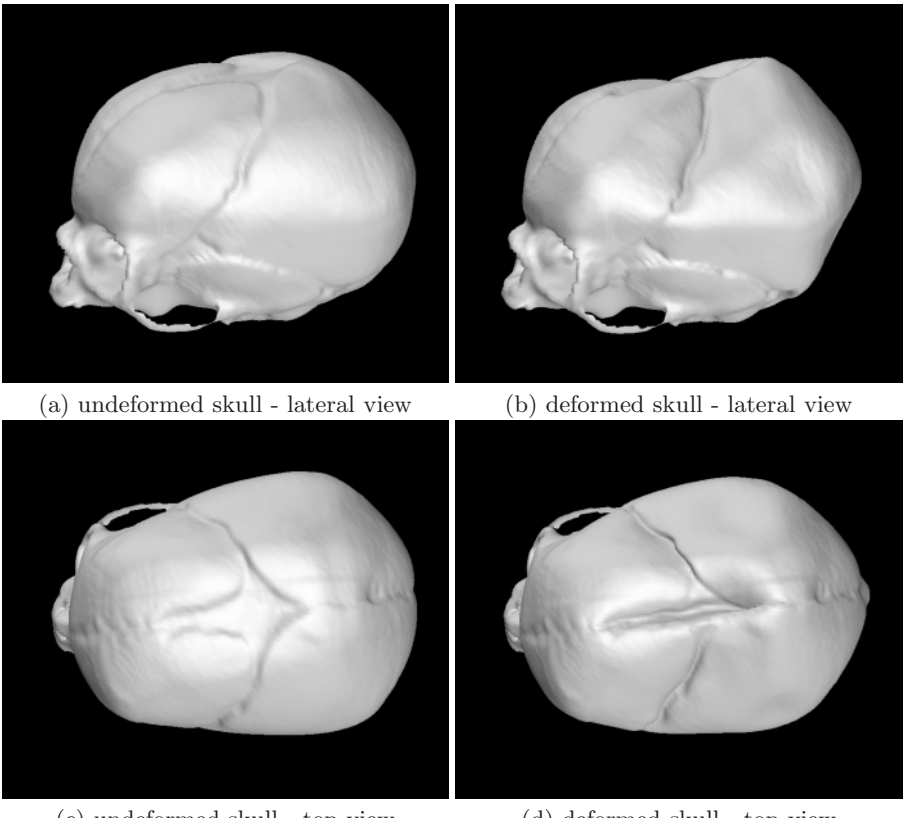

(a) undeformed skull - lateral view (b) deformed skull - lateral view

(c) undeformed skull - top view (d) deformed skull - top view

Fig. 6. Fetal skull before and after moulding (deformation magnification = 10).

Acknowledgements

We wish to thank Dr. Robin Richards from the Dept. of Medical Physics at UCL for his help (and patience) to obtain the laser-scan data of the fetal skull model.

References

1. F. Bell. *The bio-mechanics of human parturition: A fundamental approach to the mechanics of the first stage of labour*. PhD thesis, University of Strathclyde - Glasgow, 1972. 1143
2. L. Lindgren and C.N. Smyth. Measurement and interpretation of the pressures upon the cervix during normal and abnormal labour. *J.Obstet.Gynaec.Brit.Cwlth*, 68:901–915, 1961. 1143, 1149
3. A. Rempen and M. Kraus. Pressures on the fetal head during labour. *J.Perinat.Med*, (19):199–206, 1991. 1143, 1149

4. M.C. Antonucci et al. Simultaneous monitoring of the head-to-cervix, intrauterine pressure and cervical dilatation during labour. *Med.Eng.Physics*, 19(4):317–326, 1997. 1143, 1149
5. A. Wischnik et al. Zur prävention des menschlichen geburtstraumas i.mitteilung: Die computergestützte simulation des geburtsvorganges mit hilfe der kernspin-tomographie und der finiten-element-analyse. *Geburtshilfe und Frauenheilkunde*, 53:35–41, 1993. 1144
6. W.E. Lorensen and H.E. Cline. Marching cubes, a high resolution 3d surface construction algorithm. *Computer Graphics*, 21(4), 1987. 1144
7. B. Geiger. *Three-dimensional modeling of human organs and its application to diagnosis and surgical planning*. PhD thesis, Ecole des Mines de Paris, April 1993. 1144
8. Y. Liu, M. Scudder, and M.L. Gimovsky. Cad modeling of the birth process part ii. In H. Sieburg, S. Weghorst, and K. Morgan, editors, *Health Care in the Information Age*, pages 652–666. IOS Press and Ohmsha, 1996. 1144
9. G.K. McPherson and T.J. Kriewall. The elastic modulus of fetal cranial bone: A first step towards an understanding of the biomechanics of fetal head moulding. *Journal of Biomechanics*, (13):9–16, 1980. 1144, 1148, 1152, 1153
10. G.K. McPherson and T.J. Kriewall. Fetal head molding : An investigation utilizing a finite element model of the fetal parietal bone. *Journal of Biomechanics*, (13):17–26, 1980. 1144, 1148, 1149, 1152
11. R.R. Hosey and Y.K. Liu. A homeomorphic finite element model of the human head and neck. In R.H. Gallagher et al., editor, *Finite Elements in Biomechanics*. John Wiley and Sons, Binghamton USA, 1982. 1144
12. A.D. Linney et al. Three-dimensional visualization of computerized tomography and laser scan data for the simulation of maxillo-facial surgery. *Medical Informatics*, 14(2):109–121, 1989. 1144
13. F.L. Bookstein. *Morphometric tools for landmark data*. Cambridge University Press, New-York, 1991. 1146
14. S.H. Lo. A new mesh generation scheme for arbitrary planar domains. *Int.J.Num.Meth.Eng*, 21:1403–1426, 1985. 1146
15. NAFEMS. *A Finite Element Primer*. National Agency for Finite Element Methods and Standards, Glasgow, Schotland, 1987. 1146
16. K-J. Bathe. *Finite Element Procedures*. Prentice-Hall, Englewood Cliffs, New-Jersey, 1996. 1146
17. R.J. Lapeer and R.W. Prager. 3d shape recovery of a newborn skull using thin-plate splines. *Computerized Medical Imaging and Graphics*. In Press. 1147
18. R.D. Cook. *Finite Element Modeling for Stress Analysis*. John Wiley, USA, 1995. 1147
19. J.H. McElhaney et al. Mechanical properties of cranial bone. *Journal of Biomechanics*, 3:495–511, 1970. 1148
20. B. Sorbe and S. Dahlgren. Some important factors in the molding of the fetal head during vaginal delivery - a photographic study. *Int.J.Gynaecol.Obstet.*, (21):205–212, 1983. 1150, 1151, 1152, 1153
21. D.L. Bylski, T.J. Kriewall, et al. Mechanical behaviour of the fetal dura mater under large deformation biaxial tension. *J.Biomechanics*, 19(1):19–26, 1996. 1151, 1152
22. Y.C. Fung. *Biomechanics*. Springer-Verlag, USA, 1993. 1152
23. P. Govaert. *Cranial Haemorrhage in the Term Newborn Infant*. Mac Keith Press - Cambridge University Press, London, 1993. 1152